International Journal of Heat and Fluid Flow 000 (2016) 1–7

Contents lists available at ScienceDirect

International Journal of Heat and Fluid Flow

journal homepage: www.elsevier.com/locate/ijheatfluidflow

Experimental and numerical investigation of a strongly-forced precessing cylinder flow

Thomas Albrecht[a,*], Hugh M. Blackburn[a], Patrice Meunier[b], Richard Manasseh[c], Juan M. Lopez[d]

[a] Department of Mechanical and Aerospace Engineering, Monash University, VIC 3800, Australia
[b] IRPHE, CNRS, and Aix–Marseille Université, 49 Rue Joliot-Curie, 13013 Marseille, France
[c] Department of Mechanical and Product Design Engineering, Swinburne University of Technology, VIC 3122, Australia
[d] School of Mathematical and Statistical Sciences, Arizona State University, Tempe, AZ 85287, USA

ARTICLE INFO

Article history:
Available online xxx

Keywords:
Precession
Inertial waves
Instability
Symmetry breaking
Triadic resonance
PIV
DNS

ABSTRACT

Planar particle image velocimetry (PIV) and direct numerical simulations (DNS) of the flow in a precessing cylinder of height-to-radius ratio of 1.835 are presented for a nutation angle of 15° and a Reynolds number 6430 based on the cylinder's angular frequency. We find excellent agreement in terms of time-averaged velocity profiles and Kelvin mode amplitudes during the initial development and in the asymptotic state. In the experiment, a rapid transition to a disordered state follows a brief appearance of azimuthal structures with a predominant wavenumber $m = 9$. In the DNS, the transition occurs later than in the experiment, and shows dominance of a triad of azimuthal wavenumbers $m = 1, 4, 5$ during the transient evolution. Adding a small random perturbation to the simulation after the forced mode is established accelerates transition to flow dominated by $m = 9$ which eventually transitions to a disordered state, consistent with observations from PIV. The breaking of rotoreflection (inversion) symmetry of the system is found to be critical in establishing evolution paths to the disordered and asymmetric asymptotic state.

© 2016 Elsevier Inc. All rights reserved.

1. Introduction and background

Rotating flows are present in the atmosphere, in oceans and lakes, in astrophysical and many technical applications. A rotating system allows for inertial waves to exist owing to the restoring effect of the Coriolis force. One way to excite inertial waves is precession, the simultaneous rotation around two axes as sketched in Fig. 1: a cylinder of radius R and height H, tilted through an angle α and rotating at an angular frequency Ω_1, is mounted on a turntable which rotates at Ω_2. Precession is considered as a possible driver for the geo-dynamo, i.e. the creation of Earth's magnetic field (Malkus, 1968; Giesecke et al., 2015, and references therein). Also, liquid fuel in spin-stabilised spacecraft may be subject to precessional forcing, destabilising the whole spacecraft (Manasseh, 1993).

Some types of instability and transition of rotating flows may be associated with Kelvin modes, the linear, inviscid eigenmodes of solid-body rotation flow. Although not solutions of the full Navier–Stokes equations with no-slip boundary conditions, at sufficiently large Reynolds number they can be useful diagnostics of experimental and numerical observations in contained flows. In addition, they have served as the basis of a theoretical model for a triadic resonance instability mechanism which has been shown to work well in modelling behaviour in the weakly nonlinear regime within a cylinder, near onset of instability in the presence of weak precessional forcing (Albrecht et al., 2015; Meunier et al., 2008). In the present work we have used planar projections onto low-order Kelvin modes as one basis for comparison of large-scale energetics from experiment and DNS, though their utility is limited in attempting to completely describe flows in the strongly forced (and ultimately disordered) regime, which is the focus of our attention. We note, however, that triadic resonance mechanisms may still exist even when Kelvin mode descriptions are inadequate; the minimum requirement is that azimuthal wavenumbers and temporal frequencies of participating structures satisfy the triad conditions (see Section 2.3 Albrecht et al., 2015). For example, in a precessing cylinder, the directly forced flow has fundamental azimuthal

* Corresponding author. Tel.: +61435015543.
E-mail addresses: thomas.albrecht@monash.edu (T. Albrecht), hugh.blackburn@monash.edu (H.M. Blackburn), meunier@irphe.univ-mrs.fr (P. Meunier), rmanasseh@swin.edu.au (R. Manasseh), jmlopez@asu.edu (J.M. Lopez).

http://dx.doi.org/10.1016/j.ijheatfluidflow.2016.05.009
0142-727X/© 2016 Elsevier Inc. All rights reserved.

Please cite this article as: T. Albrecht et al., Experimental and numerical investigation of a strongly-forced precessing cylinder flow, International Journal of Heat and Fluid Flow (2016), http://dx.doi.org/10.1016/j.ijheatfluidflow.2016.05.009

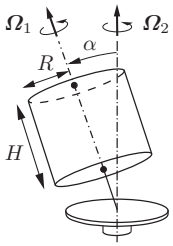

Fig. 1. Schematic of precessional forcing: a cylinder of radius R and height H, rotating at $\boldsymbol{\Omega_1}$, is tilted through a nutation angle α and is mounted on a turntable which rotates at $\boldsymbol{\Omega_2}$.

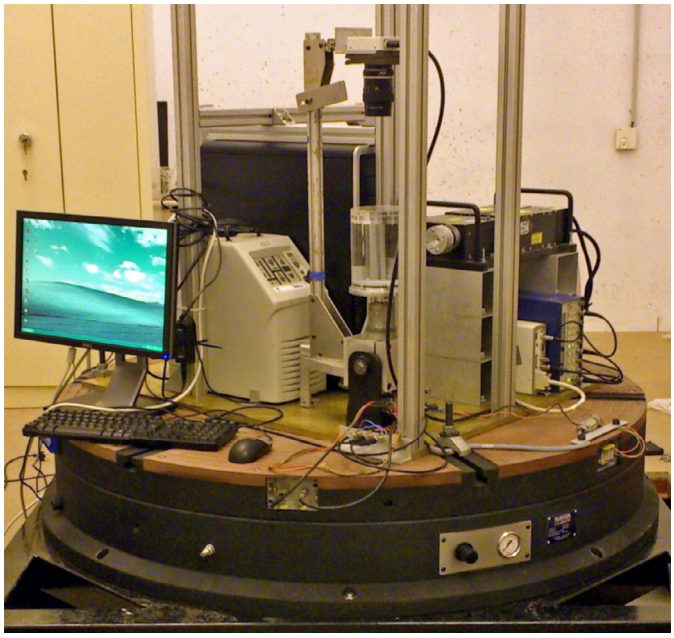

Fig. 2. Experimental setup: water-filled cylinder, PIV camera, laser and computer, all mounted on a rotating table.

wavenumber $m = 1$, so that the azimuthal wavenumbers of other structures participating in a triad instability with this component must sum to unity.

2. Experimental set-up and PIV procedure

Fig. 2 shows the experimental set-up. A cylinder, filled with water and spinning at $\boldsymbol{\Omega_1}$, is mounted on a DC motor's axis. A rotary encoder measures the motor's angular velocity with an accuracy of 0.1%. The cylinder is made from Perspex and has an inner radius $R = 46.2\text{mm} \pm 0.1\text{mm}$. Its effective height H can be varied by using different inserts. Aligned with the axis and facing the cylinder's top, a Redlake ES 11000 11-megapixel camera records PIV images. Motor, cylinder and camera are mounted on a gimbal which can be tilted to an angle α of up to 15° using a linear stepper motor. The accuracy of the tilt angle is 0.1°. A light sheet created by a 250 mJ dual-pulse NdYAG laser (Big Sky Laser) and cylindrical lenses illuminates a cross-section of the tilted cylinder at a height z_{PIV}. The coordinate system is fixed at the centre of the cylinder. Together with a PC controlling the camera, all of the above is mounted on a large platform rotating at $\boldsymbol{\Omega_2}$.

The total angular velocity along the axis of the cylinder in the inertial frame of reference is

$$\Omega = \Omega_1 + \Omega_2 \cos\alpha. \tag{1}$$

Initially, the cylinder was spinning upright (i.e. with $\alpha = 0$) to establish a solid-body rotation. It was then tilted (defining $t = 0$)

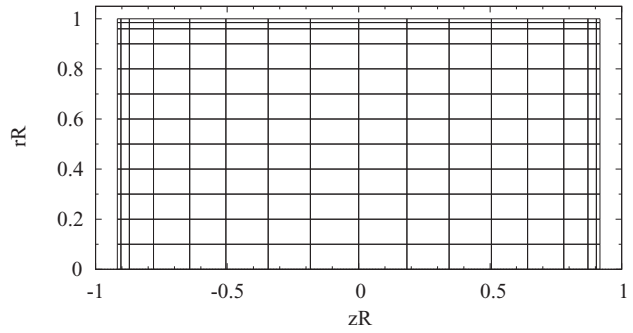

Fig. 3. Spectral element mesh of the meridional semi-plane for a cylinder of height:radius ratio $\Gamma = 1.835$.

and 200 image pairs (the maximum permitted by available memory) of the transient flow were recorded at 1Hz. An image pair had a time separation of $\Delta t = 11\,\text{ms}$, during which the cylinder turned approximately 2°. The PIV resolution was 0.0419 mm/px. Grid refinement (final window size 64×64 px), a 50% image overlap, and image shifting were applied. The seeding particles (Optimage Ltd) had a nominal diameter of $30\,\mu\text{m}$ and a density of $1 \pm 0.02\,\text{kg/m}^3$.

Since the camera is mounted in the gimbal frame of reference, it mainly records solid-body rotation flow. To extract the secondary flow, we subtract the cylinder rotation by counter-rotating the image pairs prior computing the PIV cross-correlation. For this, it is essential to know the exact centre of rotation in image coordinates since errors in its position, $\Delta\boldsymbol{x}_c$, introduce a spurious mean velocity $\sim \Delta\boldsymbol{x}_c/\Delta t$. We found that the centre of rotation in image coordinates could differ between experiments (when the cylinder was removed and replaced) or even move during one experiment (during the tilting, although the cause of the centre shift remains unclear). We therefore adopted a mostly automatic procedure to obtain the centre of rotation for each experiment individually, consisting of: (*i*) iteratively identifying the cylinder wall at eight azimuthal locations by finding radial step changes of image brightness averaged over segments of 15°, (*ii*) fitting an ellipse to the eight wall locations, and (*iii*) time-averaging the centre to eliminate wobbling due to a slight misalignment of cylinder axis and its rotation axis.

3. Computational method

The computational methodology is similar to that employed in Albrecht et al. (2015), with a cylindrical coordinates spectral element–Fourier method for the incompressible Navier–Stokes equations (Blackburn and Sherwin, 2004), solved in a reference frame which after tilt-over rotates steadily with angular velocity $\boldsymbol{\Omega_2}$. The system was non-dimensionalised using the cylinder radius R as the length scale, and the cylinder rotation rate $1/\Omega_1$ as the time scale. The cylindrical coordinates are $\boldsymbol{r} = (r, \varphi, z)$ and the corresponding velocity is $\boldsymbol{u} = (u, v, w)$. The non-dimensional governing equations are

$$\frac{\partial \boldsymbol{u}}{\partial t} + \boldsymbol{u}\cdot\nabla\boldsymbol{u} + \frac{2}{\Omega_1}\boldsymbol{\Omega_2}\times\boldsymbol{u} + \frac{1}{\Omega_1}\frac{\mathrm{d}\boldsymbol{\Omega_2}}{\mathrm{d}t}\times\boldsymbol{r} = -\nabla p + \frac{1}{Re}\nabla^2\boldsymbol{u},$$
$$\text{with} \quad \nabla\cdot\boldsymbol{u} = 0, \tag{2}$$

where any terms that can be written as gradients of a scalar are absorbed into the pressure gradient term, and p is the reduced pressure. The results presented below were computed in the gimbal frame of reference, in which the boundary conditions on all cylinder walls are $u = w = 0$ and $v = r$, and the initial condition is solid-body rotation, $(u, v, w) = (0, r, 0)$.

The spectral element mesh used had 192 spectral elements covering the meridional semi-plane, as shown in Fig. 3, and 128 data planes (64 Fourier modes) in azimuth. Local mesh refinement is

Please cite this article as: T. Albrecht et al., Experimental and numerical investigation of a strongly-forced precessing cylinder flow, International Journal of Heat and Fluid Flow (2016), http://dx.doi.org/10.1016/j.ijheatfluidflow.2016.05.009

Download English Version:

https://daneshyari.com/en/article/4993271

Download Persian Version:

https://daneshyari.com/article/4993271

Daneshyari.com